JOURNAL OF BIOMOLECULAR STRUCTURE AND DYNAMICS
https://doi.org/10.1080/07391102.2020.1763201

An investigation into the identification of potential inhibitors of SARS-CoV-2 main protease using molecular docking study

Sourav Das[#], Sharat Sarmah[#], Sona Lyndem and Atanu Singha Roy

Department of Chemistry, National Institute of Technology Meghalaya, Shillong, India

Communicated by Ramaswamy H. Sarma

ABSTRACT

A new strain of a novel infectious disease affecting millions of people, caused by severe acute respiratory syndrome coronavirus 2 (SARS-CoV-2) has recently been declared as a pandemic by the World Health Organization (WHO). Currently, several clinical trials are underway to identify specific drugs for the treatment of this novel virus. The inhibition of the SARS-CoV-2 main protease is necessary for the blockage of the viral replication. Here, in this study, we have utilized a blind molecular docking approach to identify the possible inhibitors of the SARS-CoV-2 main protease, by screening a total of 33 molecules which includes natural products, anti-virals, anti-fungals, anti-nematodes and anti-protozoals. All the studied molecules could bind to the active site of the SARS-CoV-2 protease (PDB: 6Y84), out of which rutin (a natural compound) has the highest inhibitor efficiency among the 33 molecules studied, followed by ritonavir (control drug), emetine (anti-protozoal), hesperidin (a natural compound), lopinavir (control drug) and indinavir (anti-viral drug). All the molecules, studied out here could bind near the crucial catalytic residues, HIS41 and CYS145 of the main protease, and the molecules were surrounded by other active site residues like MET49, GLY143, HIS163, HIS164, GLU166, PRO168, and GLN189. As this study is based on molecular docking, hence being particular about the results obtained, requires extensive wet-lab experimentation and clinical trials under *in vitro* as well as *in vivo* conditions.

ARTICLE HISTORY
Received 18 April 2020
Accepted 27 April 2020

KEYWORDS
SARS-CoV-2 M^{pro}; molecular docking; natural products; anti-virals; anti-fungals

1. Introduction

The recent outbreak of a novel coronavirus disease (COVID-19), occurring from a severe acute respiratory syndrome (SARS) like coronavirus started in Wuhan, China, is spreading rapidly in humans, which is now considered as a global pandemic (Lu et al., 2020). WHO, on 30 January 2020, declared this outbreak as Public Health Emergency of International Concern and later on 11 February 2020 named it as COVID-19 ("Coronavirus (COVID-19) events as they happen," 2020). According to the data of WHO (https://www.who.int/emergencies/diseases/novel-coronavirus-2019/situation-reports), currently (as on 24th April 2020), more than 2.6 million COVID-19 cases have been confirmed globally, and the number of death toll rose to 1,81,938 which are increasing exponentially. To date no specific medications have been developed, and therefore considering the risk factors associated with this disease, there is an urgent need for a treatment method to treat this disease in order to limit the transmission (Enayatkhani et al., 2020). Among all the treatment strategies, the uses of already known viral medications have great advantages as the pharmacokinetics, pharmacodynamics, and safety profiles of these drugs have already been established. This drug repurposing strategy has gained significance as they are expected to be faster with less investment (Fitchett et al., 2014; Law et al., 2013; Pant et al., 2020; Park, 2019). Preliminary studies revealed Lopinavir/ritonavir combined therapy as a potential inhibitor of the virus. Along with these two drugs, many other antiviral drugs have also been screened (Lu, 2020; Y. Wang et al., 2020; Xu et al., 2020). Recently, anti-malarial drug chloroquine (M. Wang et al., 2020) and hydroxychloroquine (Gautret et al., 2020) have been reported to have certain curative effect on COVID-19. Due to diverse bioactivity and less toxicity, naturally occurring bioactive flavonoid molecules have also been screened for their potential therapeutic effects (Khaerunnisa et al., 2020; Thuy et al., 2020). Numerous reports to identify the potential inhibitors of novel coronavirus (COVID-19) have recently been published using computational methods (Aanouz et al., 2020; Elmezayen et al., 2020; Gupta et al., 2020; Muralidharan et al., 2020; Sarma et al., 2020). The transcription of the genomic RNA inside the cell generates a polypeptide which is proteolytically cleaved by the main protease (M^{Pro} which is also known as $3CL^{Pro}$ or chymotrypsin-like protease) at 11 different sites to produce proteins necessary for the replication of the virus. Inhibition of the activity of the main protease is expected to block the viral replication as no human proteases are known having similar cleavage specificity (Boopathi et al., 2020; Zhang et al., 2020). Therefore M^{Pro} is one of the most explored drug target among the corona viruses that plays a major role in the translation and

CONTACT Atanu Singha Roy singharoyatanu@gmail.com Department of Chemistry, National Institute of Technology Meghalaya, Shillong 793003, India
[#]Equal contribution.

Supplemental data for this article can be accessed online at https://doi.org/10.1080/07391102.2020.1763201.

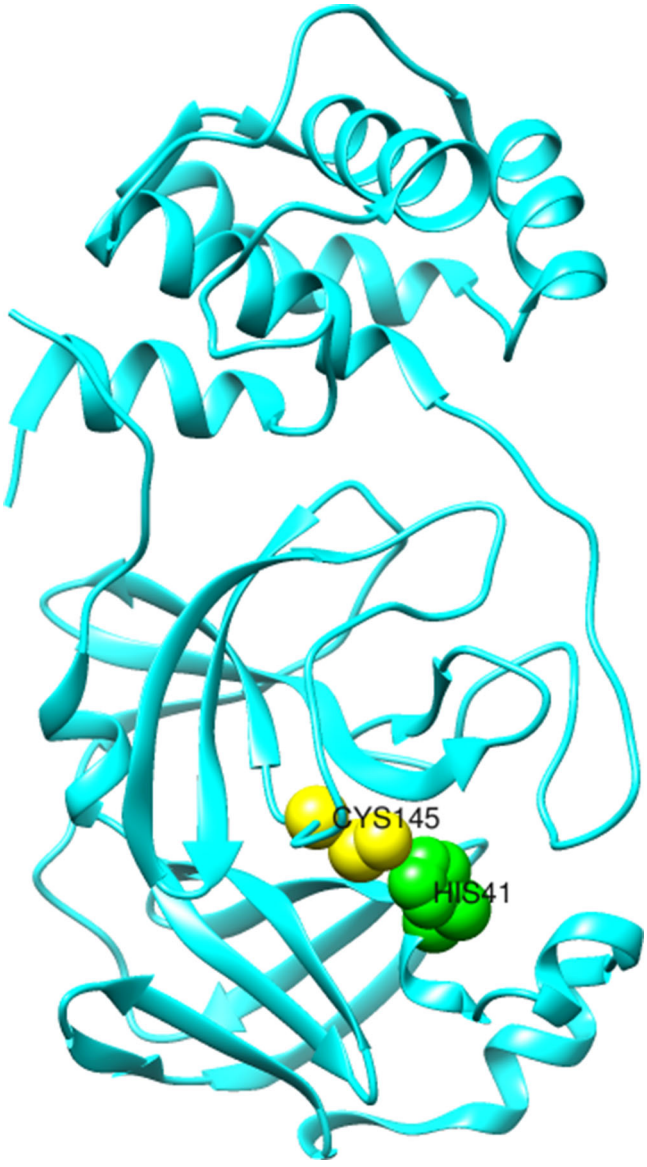

Figure 1. Crystal structure of a single chain of SARS-CoV-2 main protease (PDB:6y84) indicating the amino-acid residues of the catalytic site, HIS41 and CYS145 as green and yellow spheres, respectively.

replication of new generation viruses from the viral genomic RNA (Morse et al., 2020; Wu et al., 2006). Many crystal structures of M^{Pro} of SARS-CoV-2 have already been submitted to protein data bank (PDB) which are in both liganded and unbounded form (Jin et al., 2020; Owen et al., 2020; Zhang et al., 2020). The 3 D structure of SARS-CoV-2 M^{pro} (PDB ID. 6Y84), is made up of three domains, where domain I, II and III spans across 8-101, 102-184 and 201-306 amino acid residues, repectively. Domain I and II mainly consists of β-barrels while domain III mainly consists of α-helices (S. A. Khan et al., 2020). The substrate/active site of binding is located at the cleft of domain I and II, which consists of two catalytic residues, namely, HIS41 and CYS145 (Figure 1).

Here in this report, a total of 33 compounds belonging to different classes (i) control drugs, (ii) natural products, (iii) anti-virals, (iv) anti-fungals, (v) anti-nematodes and anti-protozoal were identified to investigate their inhibitory effects towards M^{Pro} by molecular docking analysis. Ritonavir, hydroxychloroquine, penciclovir and lopinavir are known drugs that have been screened for the treatment of COVID-19. The reason for them being used as control drugs in the study is that, as mentioned earlier, lopinavir/ritonavir combination, and anti-malarial drug hydroxychloroquine has recently been found to be a potential inhibitor of the virus, while penciclovir could also inhibit the virus to some extent (M. Wang et al., 2020). Considering the diverse pharmaceutical properties of the natural products including anti-viral properties (Jo et al., 2020; Thayil & Thyagarajan, 2016; Zakaryan et al., 2017), a total of 17 compounds: curcumin, demethoxycurcumin, (-)-Epigallocatechin gallate (EGCG), (-)-epigallocatechin, (EGC), hesperidin, myricitrin, puerarin, scutellarin, rutin, quercitrin, capsaicin, ursolic acid, glabridin, apiin, rhoifolin, glycyrrhizin, and vitexin were screened for their inhibitory potential against SARS-CoV-2 M^{pro}. Azidothymidine, indinavir, tipranavir, and saquinavir are the well-known anti-viral drugs (De Clercq & Li, 2016), while diethylcarbamazine, primaquine, mepacrine, artemisinin and niclosamide are the anti-nematodes (Panic et al., 2014) and emetine, an anti-protozoal drug (Akinboye & Bakare, 2011), which have also been screened for their inhibitory potentials. Further, two anti-fungals, namely, fluconazole and itraconazole (Vardakas et al., 2005) were also docked to the main protease of COVID-19. This study is focused on the repurposing/identification of compounds with a sole aim to expedite the identification of specific drugs for the treatment of COVID-19.

2. Materials and methods

Molecular docking methods are the best tools to predict the drug interactions with macromolecules. The blind docking method involves a search throughout the entire surface of the macromolecule for binding sites. Therefore, blind molecular docking analyses of some known drugs along with some bioactive natural compounds, have been screened with the main protease of COVID-19, SARS-CoV-2 M^{pro}.

2.1. Optimization of the 3 D coordinates of the ligands

The 3 D coordinates of the ligands, ritonavir (347980), hydroxychloroquine (3526), penciclovir (4563), lopinavir (83706), curcumin (839564), demethoxycurcumin (4579941), (-)-epigallocatechin gallate, EGCG (58575), (-)-epigallocatechin, EGC (65231), hesperidin (10176), myricitrin (4444992), puerarin (4445119), scutellarin (161366), rutin (4444362), quercitrin (4444112), capsaicin (1265957), ursolic acid (58472), glabridin (110560), apiin (4444321), rhoifolin (4445347), glycyrrhizin (14263), vitexin (4444098), azidothymidine (32555), indinavir (4515036), tipranavir (10482313), saquinavir (390016) and emetine (9802). Diethylcarbamazine (2944), primaquine (4739), mepacrine (232), artemisinin (62060) and niclosamide (4322) and emetine (9802) were obtained from ChemSpider (www.chemspider.com) as a .mol file and further geometry optimization was carried out in ArgusLab using PM3 methods (Thompson, 2004). The optimized structures of the ligands are shown in Figure S1. The

code within the parenthesis signifies the ChemSpider ID of the respective molecules.

2.2. Drug like properties of the ligands

The drug likeliness of a molecule is indicated by the Lipinski's rule of five parameters (molecular weight <500 Da, no more than 5 hydrogen bond donors, no. of hydrogen bond acceptors should be less than 10 and log*P* should not be greater than 5). The Lipinski's rule of five parameters were obtained from the SWISSADME server (www.swissadme.ch/index.php) (Daina et al., 2017). The chemical structures, chemical formula and the Lipinski's rule parameters of the ligands are listed in Table S1 (Supplementry Information).

2.3. Structure and preparation of M^{Pro} for docking studies

The crystal structure of M^{Pro} (PDB ID: 6Y84) was obtained from Protein Data Bank (PDB) (Owen et al., 2020). The obtained structure was a dimer of two homologous amino acid chains (A and B). The chain A was used for molecular docking. Water molecules were removed from the PBD using PyMOL (Schrodinger LLC, 2017).

2.4. Molecular docking analyses and visualization

The final PDB file of the protease and geometry optimized ligand structures were selected for molecular docking analyses in the SwissDock server (http://www.swissdock.ch/docking). SwissDock is based on EADock DSS docking software which estimates the CHARMM (Chemistry at HARvard Macromolecular Mechanics) energy on a grid and the most favourable binding modes are clustered in the server (Grosdidier et al., 2011). The docked pose with the minimum fullfitness score is considered for futher analysis. UCFS Chimera (Pettersen et al., 2004), a molecular visualization tool, was used to visualize the results obtained from the server. Discovery Studio Visualizer was further employed in order to prepare the docked poses and 2 D interaction plots (Biovia, 2019). The changes in the accessible surface area of the SARS-CoV-2 M^{pro} protease upon ligand binding were determined using an online server (http://cib.cf.ocha.ac.jp/bitool/ASA/). The electrostatic surface potential was determined using the APBS plugin of PyMOL (Schrodinger LLC, 2017).

3. Results and discussion

As mentioned earlier, in addition to the control drugs for the treatment of COVID-19, here we have performed the molecular docking studies of various naturally occurring compounds, anti-virals, anti-fungals, anti-nematodes and anti-protozoal drug with SARS-CoV-2 M^{pro}. According to the SwissDock server, the binding modes of the ligands are ranked according to their fullfitness score, therefore the conformers having the minimum fullfitness score were analyzed for further evaluations. Table 1 list the fullfitness score and the free binding energy associated with each corresponding docked pose, this Table 1 will be further utilized in the following sections which rationalize the results obtained from the docking studies one by one.

3.1. Docking studies of the control drugs with SARS-CoV-2 M^{pro}

The docked pose of the minimum energy (fullfitness score) conformers of the four control drugs, namely, penciclovir, ritonavir, hydroxychloroquine and lopinavir along with their corresponding 2 D interaction plots are depicted in Figure 2. The docked poses clearly demonstrate that the drugs molecules bind within the active site of the SARS-CoV-2 M^{pro} macromolecular structure. Figure 2a shows that penciclovir binds firmly through three conventional hydrogen bonds with residues HIS41, CYS44 and GLU166 besides other interactions such as carbon-hydrogen bonds (ASN142 and MET165) and van der Waals interactions. Ritonavir binds to the active site of SARS-CoV-2 with different types of non-covalent interactions, as depicted in Figure 2b. Ritonavir stabilizes in the active site through hydrogen bonding with THR25 and SER46, π-sigma with THR26, alkyl hydrophobic with MET165, π-alkyl hydrophobic with LEU27, CYS145 and PRO168, and van der Waals interactions with other residues as depicted in the 2 D plot. Hydroxychloroquine, a promising candidate for the treatment of the current pandemic due to SARS-CoV-2 (Gautret et al., 2020), has been found to bind within the active site of the protease through π-sulphur interaction with MET165, π-sigma with GLN189, alkyl hydrophobic with LEU167 and PRO168, and van der Waals interactions with other residues as shown in Figure 2c. Similarly, lopinavir interacts with the residues in the active site through hydrogen bonding with THR26, π-sulphur interaction with CYS145 and alkyl hydrophobic with PRO168, besides van der Waals interaction with other residues as depicted in the 2 D plot (Figure 2d). The fullfitness score along with the estimated free energy (ΔG) of binding of the above mentioned drugs are listed in Table 1. If we compare in terms of the ΔG value, we can see that ritonavir has the most negative ΔG value with - 9.52 kcal/mol followed by lopinavir, then hydroxychloroquine and finally penciclovir. This can be directly correlated with the number of non-covalent interactions that these drugs undergo with the surrounding residues within the active site of SARS-CoV-2. Moreover, the stability of a particular drug within the active site is also associated with the number of π-interactions that it undergoes with the surrounding residues (Arthur & Uzairu, 2019). The electrostatic surface potential of the binding site along with the simultaneous presence of the four drugs are shown in Figure S2.

3.2. Docking studies of the natural compounds with SARS-CoV-2 M^{pro}

The docked pose of the minimum energy (fullfitness score) conformers of the 17 natural products, namely, curcumin, demethoxycurcumin, EGCG, EGC, hesperidin, myricitrin, puerarin, scutellarin, rutin, quercitrin, capsaicin, ursolic acid,

Table 1. Fullfitness score and estimated change in free energy of the minimum docked pose of the respective possible inhibitors with SARS-CoV-2 M^{pro}.

S. No	Category	Compounds	Fullfitness score (kcal/mol)	Estimated ΔG (kcal/mol)
1	Control Drugs	Penciclovir	−1314.77	−6.57
		Ritonavir	−1313.38	−9.52
		Hydroxychloroquine	−1236.76	−7.75
		Lopinavir	−1238.78	−9.00
2	Naturally occurring compounds	Curcumin	−1236.50	−8.15
		Demethoxycurcumin	−1248.77	−7.87
		EGCG	−1232.32	−7.96
		EGC	−1237.73	−7.30
		Hesperidin	−1106.07	−9.02
		Myricitrin	−1162.12	−7.85
		Puerarin	−1166.80	−8.43
		Scutellarin	−1162.19	−8.32
		Rutin	−1100.25	−9.55
		Quercitrin	−1168.95	−8.26
		Capsaicin	−1271.85	−8.12
		Ursolic acid	−1205.16	−7.84
		Glabiridin	−1225.76	−7.59
		Apiin	−1113.95	−8.74
		Rhoifolin	−1112.70	−8.37
		Glycyrrhizin	−1068.56	−7.81
		Vitexin	−1184.31	−7.82
3	Anti-fungal drugs	Fluconazole	−1264.51	−7.49
		Itroconazole	−1168.54	−9.05
4	Anti-viral drugs	Azidothymidine	−1324.25	−7.40
		Indinavir	−1145.37	−8.84
		Tipranavir	−1219.41	−8.42
		Saquinavir	−1222.79	−8.35
5	Anti-nematodal and anti-protozoal drugs	Diethylcarbamazine	−1272.14	−6.90
		Primaquine	−1219.07	−7.45
		Mepacrine	−1227.84	−7.80
		Artemisinin	−1233.81	−7.15
		Niclosamide	−1254.12	−6.77
		Emetine	−1230.03	−9.07

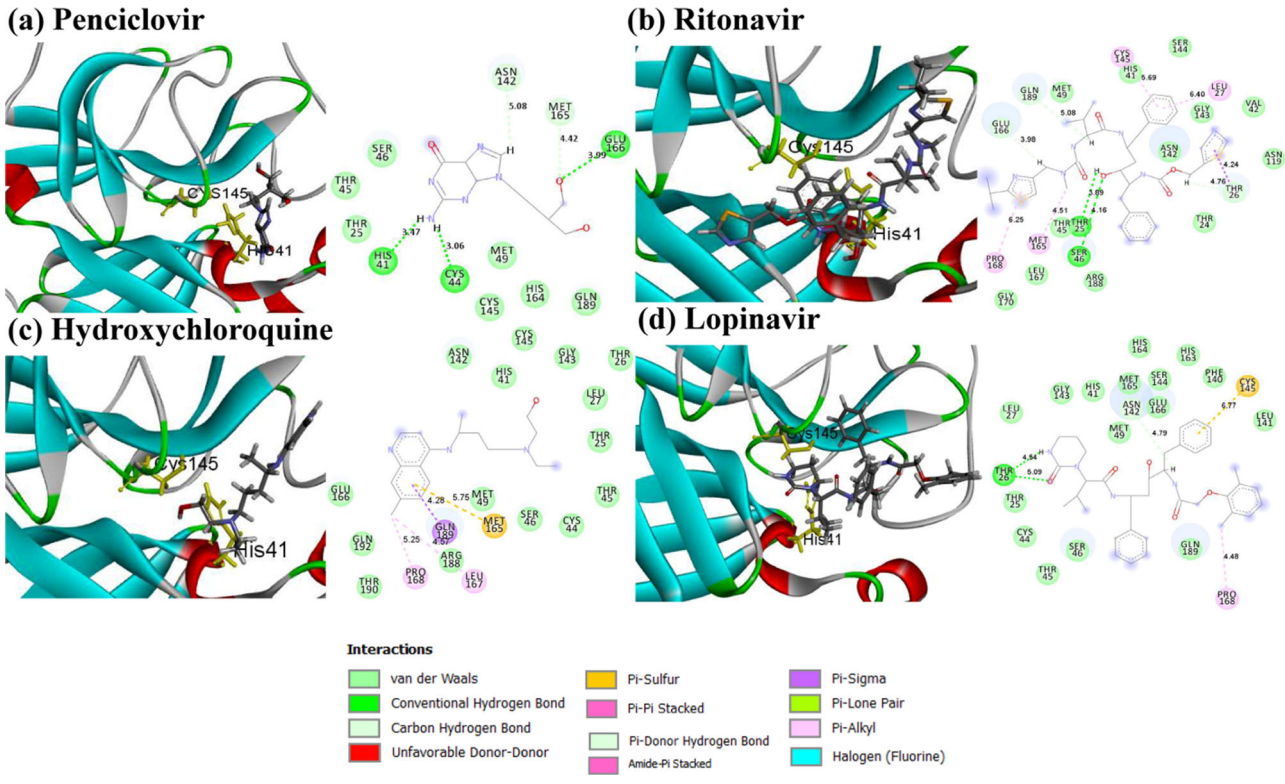

Figure 2. The minimum docked poses of the four control drugs along with their corresponding 2 D interaction plots within the active site of SARS-CoV-2 M^{pro}.

glabridin, apiin, rhoifolin, glycyrrhizin, vitexin along with their corresponding 2 D interaction plots are depicted in Figure 3. Curcumin, a potent bioactive molecule binds in the active site of SARS-CoV-2 M^{pro} (Figure 3a) through hydrogen bonding with GLY143 and GLN192, π-sulphur, π-sigma interactions with CYS145 and PRO168, respectively, along with other non-covalent interactions such as van der Waals interactions with other residues as shown in the 2 D plot (Figure

3a). EGC, a tea polyphenol, binds to the active site through hydrogen bonding with THR26, HIS41 and ASN142, and van der Waals forces with other residues (Figure 3b). Demethoxycurcumin binds in the active site (Figure 3c) through hydrogen bonding with CYS44 and PRO168, π-sigma with PRO168 and π-alkyl with MET49. Hesperidin interacts through hydrogen bonding with THR24, THR25, THR45, HIS4, SER46, CYS145, amide-π stacked interaction with THR45, π-alkyl interactions with MET49 and CYS145 (Figure 3d). EGCG interacts with PHE140, GLU166, GLN192 through hydrogen bonding, CYS145 through π-sulphur, GLN189 through π-sigma and other non-covalent forces as depicted in the 2 D plot of Figure 3e. Myricitrin stabilizes in the active site mainly through hydrogen bonding with the THR24, THR25, THR26, ASN119, ASN42 residues as shown in Figure 3f, while puerarin gets stabilized by hydrogen bonding with HIS41, CYS44, GLY143 and GLU166 residues (Figure 3g). Quercitrin, on the other hand, gets stabilized by hydrogen bonding with THR25, GLY143 and GLU166, and amide-π stacking with THr45 along with other interactions as depicted in Figure 3h. Scutellarin (Figure 3i) forms hydrogen bonds with THR26, GLY143 and CYS145 along with a π-sulphur interaction with CYS145. Capsaicin forms hydrogen bonds with THR190 along with alkyl hydrophobic (with CYS145) and π-alkyl interactions with HIS163 and PRO168 (Figure 3j). Rutin undergoes several non-covalent interactions with the residues within the active site (Figure 3k), it gets stabilized through hydrogen bonding with HIS41, LEU141, ASN142, GLU166, THR190 and GLN192, further it undergoes π-sulphur interaction with CYS145 and π-alkyl with PRO168. Ursolic acid undergoes only van der Waals interactions with the surrounding residues as shown in Figure 3l. Vitexin forms hydrogen bonds with THR26, THR45 and GLY143, and π-sigma interaction with ASN142 (Figure 3m). Glabridin interacts through hydrogen bonding with GLY143, alkyl hydrophobic with LEU27 and CYS145, and π-alkyl with HIS41 and CYS145 (Figure 3n). Glycyrrhizin forms a hydrogen bond with THR190, alkyl hydrophobic with MET49, CYS145 and MET165, and π-alkyl with HIS41 (Figure 3o). Rhoifolin stabilizes in the active site (Figure 3p) mainly through hydrogen bonding with HIS41, CYS44, ASN119 and GLU166, alkyl, and π-alkyl hydrophobic interactions with CYS145 and HIS41, respectively. Apiin undergoes several non-covalent interactions at the active site, it forms hydrogen bonds with HIS41, SER46, GLN189, π-sigma interaction with PRO168, and π-alkyl interaction with MET165 (Figure 3q). In all the above docked pose, van der Waals play a major role in the binding processes as could be observed from the respective 2 D plots from Figure 3. On comparison of the ΔG value, which gives the estimated free energy of binding, we can infer that the binding affinity of the natural products towards SARS-CoV-2 protease follows the following order rutin (−9.55 kcal/mol).> hesperidin (−9.02 kcal/mol) > apiin (−8.74 kcal/mol) > puerarin (−8.43 kcal/mol) > Rhoifolin (−8.37 kcal/mol) > scutellarin (−8.32 kcal/mol) > quercitrin (−8.26 kcal/mol) > curcumin (8.15 kcal/mol) > capsaicin (−8.12 kcal/mol) > EGCG (7.96 kcal/mol) > demethoxycurcumin (−7.87 kcal/mol) ∼ myricitrin (−7.85 kcal/mol) ∼ ursolic acid (−7.84 kcal/mol) ∼ vitexin (−7.82 kcal/mol) ∼ glycyrrhizin (−7.81 kcal/mol) > glabridin (−7.59 kcal/mol) > EGCG (−7.30 kcal/mol). The electrostatic surface potential of the binding site along with the simultaneous presence of the 17 natural products is shown in Figure S3.

3.3. Docking studies of the anti-fungal drugs with SARS-CoV-2 M^{pro}

The docked pose of the minimum energy (fullfitness score) conformers of the two anti-fungals, namely, fluconazole and itraconazole along with their corresponding 2 D interaction plots are depicted in Figure 4. It can be seen that the two ligands bind within the active site of SARS-CoV-2. Fluconazole interacts through hydrogen bonding with GLY163 and GLU166, π-alkyl hydrophobic interactions with CYS145 and MET165, halogen (fluorine) bonding with CYS144 and van der Waals forces with other residues as depicted in the 2 D plot (Figure 4a). Another anti-fungal drug itraconazole is found to form hydrogen bonds with SER46 and GLY143, π-sulphur interaction with CYS145, alkyl hydrophobic and π-alkyl interactions with PRO168, along with van der Waals interactions as shown in the 2 D plot (Figure 4b). it can be seen from Table 1, that the ΔG value for itraconazole is more negative (−9.05 kcal/mol) as compared to that of fluconazole binding to SARS-CoV-2, which can also be seen from the number of interactions that each molecule undergoes with the active site residues. The electrostatic surface potential of the binding site along with the simultaneous presence of the two drugs is shown in Figure S4.

3.4. Docking studies of the anti-viral drugs with SARS-CoV-2 M^{pro}

The docked pose of the minimum energy (fullfitness score) conformers of the four anti-virals, namely, saquinavir, azidothymidine, indinavir, and tipranavir with SARS-CoV-2 protease along with their corresponding 2 D interaction plots are depicted in the Figure 5. It can be seen that the anti-virals bind within the active site of the SARS-CoV-2 M^{pro}. It could be observed from Figure 5a, that saquinavir interacts with the residues in the active site through hydrogen bonding with SER46, ASN142 and GLU166, π-π T-shaped interaction with HIS41, π-alkyl interaction with CYS145, and van der Waals forces of attraction with other residues as depicted in the 2 D plot. Azidothymidine forms hydrogen bonds with GLY143, CYS145 and GLU166, π-π stacked interaction with HIS41, π-alkyl hydrophobic interaction with CYS145 and van der Waals forces with other residues as shown in the 2 D plot (Figure 5b). Indinavir forms hydrogen bonds with ASN142 and CY145, π-sigma and π-sulphur interactions with MET49, π-π T-shaped interaction with HIS41, π-alkyl interaction with PRO168, and van der Waals interactions with other residues as depicted in 2 D plot (Figure 5c). Tipranavir forms hydrogen bond and halogen bond with THR24 residue, π-sulphur with MET165, π-alkyl with PRO168, alkyl hydrophobic interaction with LEU27, and van der Waals forces with other residues as vivid from the 2 D plot (Figure 5d). On comparison of the estimated ΔG values from Table 1 for the four anti-virals, we observed that indinavir has the most negative ΔG value (−8.84 kcal/mol), followed by

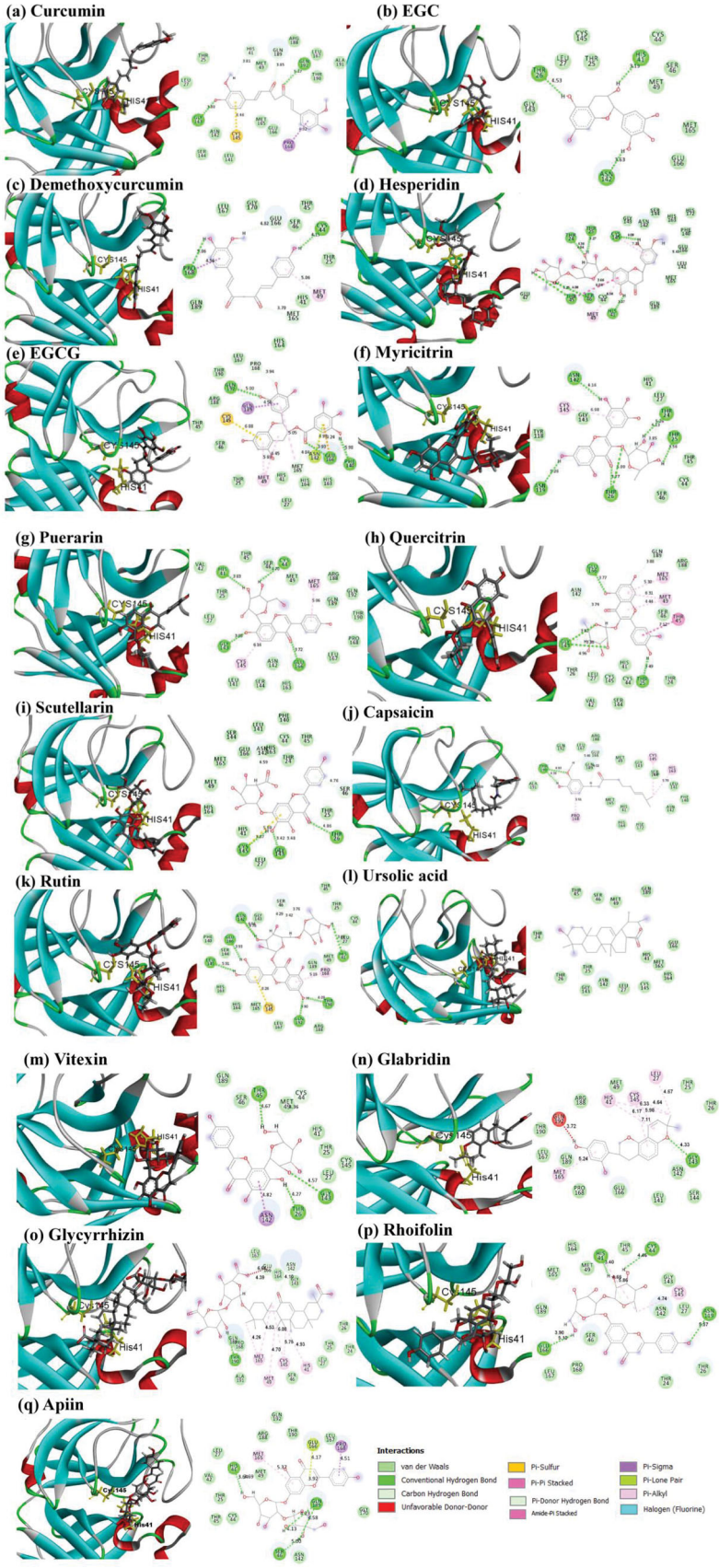

Figure 3. The minimum docked poses of the several naturally occurring compounds along with their corresponding 2 D interaction plots within the active site of SARS-CoV-2 M^{pro}.

tipranavir (−8.42 kcal/mol), saquinavir (−8.35 kcal/mol) and azidothymidine (−7.40 kcal/mol). The electrostatic surface potential of the binding site along with the simultaneous presence of the four drugs is shown in Figure S5.

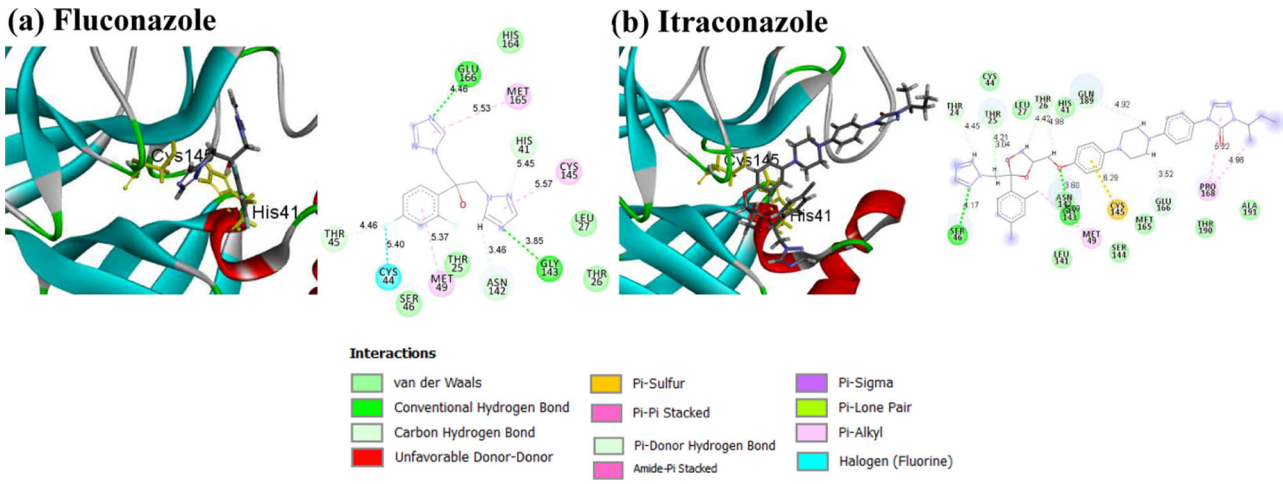

Figure 4. The minimum docked poses of two anti-fungal drugs along with their corresponding 2 D interaction plots within the active site of SARS-CoV-2 M^{pro}.

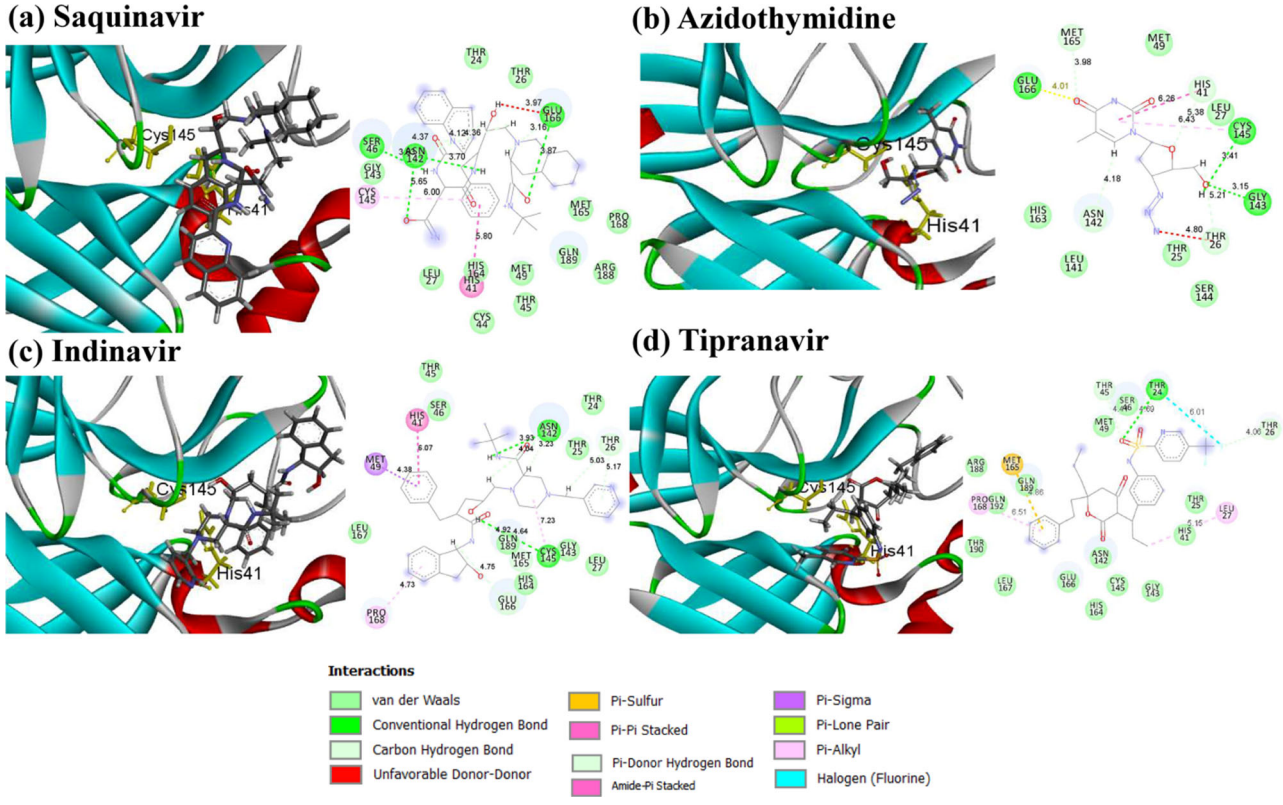

Figure 5. The minimum docked poses of anti-viral drugs along with their corresponding 2 D interaction plots within the active site of SARS-CoV-2 M^{pro}.

3.5. Docking studies of the anti-nematodal and anti-protozoal drugs with SARS-CoV-2 M^{pro}

The docked pose of the minimum energy (fullfitness score) conformers of five anti-nematodes, namely, diethylcarbamazine, primaquine, mepacrine, artemisinin and niclosamide, and one anti-protozoal drug, emetine with SARS-CoV-2 protease along with their corresponding 2 D interaction plots are depicted in Figure 6. It can be seen that the drugs bind to the active site of the SARS-CoV-2. Diethylcarbamazine (Figure 6a) interacts with LEU27, MET49 and CYS145 through alkyl hydrophobic interactions and van der Waals interaction with other residues. Primaquine (Figure 6b) forms hydrogen bond with CYS44 residue along with π-sulphur interaction with CYS145 and van der Waals interaction with other residues. Mepacrine (Figure 6c) undergoes alkyl hydrophobic interactions with CYS145 and MET165 residues, π-alkyl hydrophobic interactions with HIS163, MET165, MET49, and van der Waals interaction with other residues. Similarly, artemisinin (Figure 6d) undergoes alkyl hydrophobic interaction with MET49 and CYS145 residues along with π-alkyl interactions with HIS163. Niclosamide (Figure 6e), forms a hydrogen bond with GLY143, π-sigma and π-sulphur interactions with GLN189 and MET165, respectively, alkyl hydrophobic interactions with LEU167 and PRO168, π-alkyl interaction with CYS145. The anti-protozoal drug, emetine undergoes attractive electrostatic (salt bridge) interaction with GLU166, alkyl hydrophobic interaction with MET49, and Met165, π-alkyl

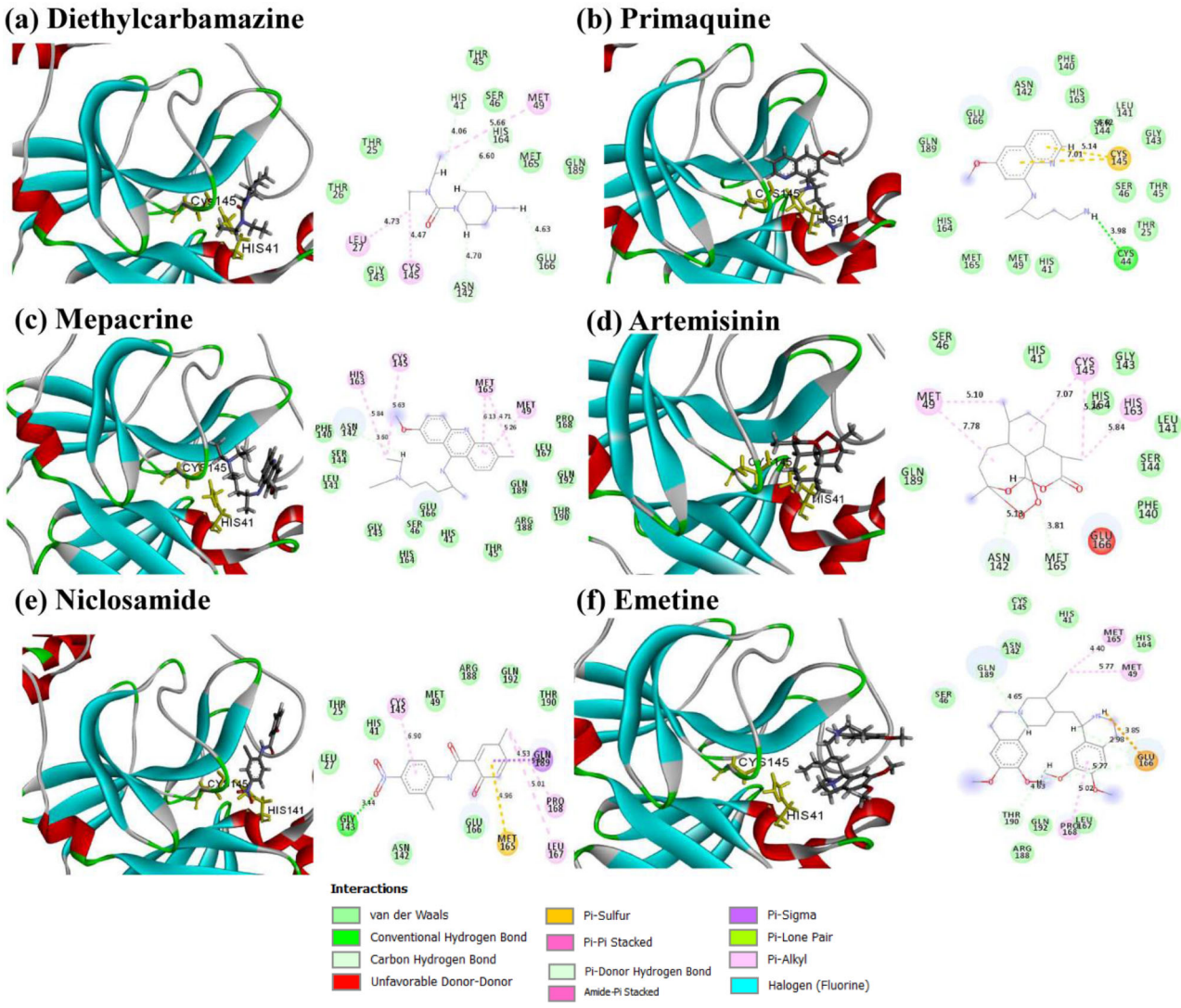

Figure 6. The minimum docked poses of anti-nematodal drugs and an anti-protozoal drug along with their corresponding 2 D interaction plots within the active site of SARS-CoV-2 M^{pro}.

interaction with PRO168 (Figure 6f). On comparison of the estimated ΔG values from Table 1 for the five anti-nematodes and one anti-protozoal, we observe that emetine has the most negative ΔG value (−9.07 kcal/mol), followed by mepacrine (−7.80 kcal/mol), primaquine(−7.45 kcal/mol), artemisinin (−7.15 kcal/mol) and finally niclosamide (−6.77 kcal/mol). The electrostatic surface potential of the binding site along with the simultaneous presence of the six drugs is shown in Figure S6.

Herein, the blind molecular docking studies carried out for a total of 33 compounds under different categories reveal that they might act as potential anti- SARS-CoV-2 drugs, as these molecules bind to the active site of the main protease of SARS-CoV-2 M^{pro}. Inhibition of this enzyme/protease is essential for blocking the viral replication (Zhang et al., 2020). This inhibitor binding site within the protease of SARS-CoV-2 consists of residues HIS41, MET49, GLY143, CYS145, HIS163, HIS164, GLU166, PRO168, and GLN189 as evident from the recent study on the α-ketoamide inhibitors for SARS-CoV-2 main protease (Zhang et al., 2020). We observe from the blind docking study of all the 33 molecules with the SARS-CoV-2 protease that the molecules are generally surrounded by the above mentioned residues, which clearly suggests that this molecule can prevent the viral replication of SARS-CoV-2. The distance of the ligands along with the change in accessible area of the two important catalytic residues (HIS41 and CYS145) within the active site of the protease is shown in Table 2. Although the blind docking studies indicates that all the molecules can act as potential agents for COVID treatments, but from the estimated free energy of binding (ΔG) values (Table 1), we can infer that rutin with the highest negative minimum ΔG value (−9.55 kcal/mol) among all the studied compounds can be the best possible SARS-CoV-2 inhibitor, followed by ritonavir (−9.52 kcal/mol), emetine (−9.07 kcal/mol), hesperidin (−9.02 kcal/mol), and indinavir (−8.84 kcal/mol).

The emergence of novel viruses requires efficient therapeutic strategies to develop or identify drugs that can treat the disease or control the further spread of the virus. In recent years, molecules that influence the life cycle of viruses have been identified, and a broad range of anti-viral agents have been proposed, which includes inhibiting the entry and

Table 2. Distance and the change in accessible surface area of the active site residues (HIS41 and CYS145) of SARS-CoV-2 M^{pro} on interaction with the potential inhibitors.

		Distance (Å)		ΔASA (Å^2)	
Category	Compounds	HIS41	CYS145	HIS41	CYS145
Control drugs	Penciclovir	3.47	4.23	20.98	16.61
	Ritonavir	3.00	5.69	21.09	18.36
	Hydroxychloroquine	2.12	3.17	21.09	15.56
	Lopinavir	3.15	6.77	21.09	21.88
Natural Products	Curcumin	3.81	6.46	21.09	21.88
	Demethoxycurcumin	4.20	4.73	18.82	10.28
	EGCG	4.12	6.68	21.09	21.88
	EGC	3.19	4.52	21.09	21.88
	Hesperidin	3.37	4.09	20.30	21.88
	Myricitrin	3.50	6.98	18.82	18.15
	Puerarin	3.83	6.16	21.09	21.88
	Scutellarin	4.30	3.87	21.09	21.88
	Rutin	3.88	8.26	21.09	21.88
	Quercitrin	3.50	4.92	21.09	21.67
	Ursolic acid	2.23	3.64	21.09	19.90
	Glabiridin	5.98	4.64	20.63	21.88
	Apiin	3.64	4.96	20.41	12.77
	Rhoifolin	3.40	4.74	21.09	15.76
	Glycyrrhizin	4.93	5.75	21.09	21.88
	Vitexin	2.08	3.54	21.09	21.36
Antifungal drugs	Fluconazole	5.45	5.57	21.09	18.77
	Itraconazole	3.50	3.46	21.09	21.88
Antiviral drugs	Azidothymidine	6.26	3.41	19.72	21.88
	Indinavir	7.23	6.07	21.09	21.88
	Tipranavir	2.66	2.69	21.09	21.78
	Saquinavir	5.80	6.00	21.09	21.46
Anti-nematodal and anti-protozoal drugs	Diethylcarbamazine	4.06	4.47	21.09	20.85
	Primaquine	3.32	5.14	19.61	19.45
	Mepacrine	3.66	5.63	18.59	19.62
	Artemisinin	4.43	5.26	20.41	21.43
	Niclosamide	3.43	6.90	20.18	21.78
	Emetine	4.09	4.59	7.93	8.73

stopping of viral replication or targeting intracellular signal transduction pathways (Elfiky & Azzam, 2020; Hasan et al., 2020). In this context, repurposing of already known drugs and molecules is an essential concept (R. J. Khan et al., 2020), especially in the pandemic that has resulted due to the novel coronavirus, as it is cost-effective in terms of research and development of new novel drug molecules. Sir James Black, the recipient of the 1988 Nobel Prize in Physiology and Medicine, had famously stated that "The most fruitful basis for the discovery of a new drug is to start with an old drug". In addition to the FDA approved drugs, here we observed that rutin and hesperidin, two dietary polyphenols have significant potential to function as inhibitors of SARS-CoV-2 M^{pro}. Dietary polyphenols have low systemic toxicity and are highly beneficial for human health (Cory et al., 2018). Rutin, also known as vitamin P, has several pharmacological properties including anti-viral activity (Ganeshpurkar & Saluja, 2017). Similarly, hesperidin has also been observed to act as an anti-viral compound (Parvez et al., 2019). Therefore, this finding also indicates a promising potential for the use of dietary polyphenols for the treatment of COVID-19.

4. Conclusion

This blind molecular docking study proposes a potential approach for the utilization of natural products, anti-virals, anti-fungals, anti-nematodal, and anti-protozoal drugs as prospective inhibitors of SARS-CoV-2 M^{pro}, a pandemic and a global threat that is currently affecting millions of people, leading to death in extreme cases. We observe that the studied bind within the active site of the 6Y84, the main protease of SARS-CoV-2, which is essential for preventing the protein mutarotation of the virus by inhibiting the viral replication, and further spread of the infection. The estimated free energy of binding varied in the range of -6.57 to -9.55 kcal/mol, suggesting the molecules can spontaneously interact within the binding site of SARS-CoV-2 M^{pro}. Among all the molecules, the inhibition activity of rutin was found to be the highest as its ΔG value (−9.55 kcal/mol) is the minimum, followed by ritonavir (−9.52 kcal/mol), emetine (−9.07 kcal/mol), hesperidin (−9.02 kcal/mol), and indinavir (−8.84 kcal/mol). As this study has been carried out using computational methods, therefore being particular about these results would require further wet-lab experiments to be carried out under *in vivo* as well as *in vitro* conditions.

Acknowledgements

The authors are grateful to National Institute of Technology Meghalaya for providing research platform. SD and SS thank TEQIP III, National Institute of Technology Meghalaya for their fellowship. The study was not supported by any funding authority. The authors thank the reviewers for their valuable suggestions to increase the scientific quality of the manuscript.

Disclosure statement

No potential conflict of interest was reported by the author(s).

Authors declaration

The authors declared that no competing conflict of interest exists. All authors have read and approved this version of the article.

Authors contribution

Sourav Das Conceptualization, Methodology, Investigation, Writing - original draft.
Sharat Sarmah Conceptualization, Methodology, Investigation, Writing - original draft.
Sona Lyndem Conceptualization, Methodology, Investigation, Writing - original draft.
Atanu Singha Roy Conceptualization, Methodology, Investigation, Writing-reviewing and editing.

References

Aanouz, I., Belhassan, A., El Khatabi, K., Lakhlifi, T., El Idrissi, M., & Bouachrine, M. (2020). Moroccan medicinal plants as inhibitors of COVID-19: Computational investigations. *Journal of Biomolecular Structure & Dynamics*. https://doi.org/10.1080/07391102.2020.1758790

Akinboye, E. S., & Bakare, O. (2011). Biological activities of emetine. *Open Natural Products Journal*, *4*, 8–15. https://doi.org/10.2174/1874848101104010008

Arthur, D. E., & Uzairu, A. (2019). Molecular docking studies on the interaction of NCI anticancer analogues with human Phosphatidylinositol 4,5-bisphosphate 3-kinase catalytic subunit. *Journal of King Saud University - Science*, *31*(4), 1151–1166. https://doi.org/10.1016/j.jksus.2019.01.011

Biovia, D. S. (2019). *Discovery studio visualizer, 2019*. Dassault Systèmes, (v19.1.0.15350).

Boopathi, S., Poma, A. B., & Kolandaivel, P. (2020). Novel 2019 coronavirus structure, mechanism of action, antiviral drug promises and rule out against its treatment. *Journal of Biomolecular Structure & Dynamics*. https://doi.org/10.1080/07391102.2020.1758788

Coronavirus (COVID-19) events as they happen. (2020). https://www.who.int/emergencies/diseases/novel-coronavirus-2019/events-as-they-happen

Cory, H., Passarelli, S., Szeto, J., Tamez, M., & Mattei, J. (2018). The role of polyphenols in human health and food systems: A mini-review. *Frontiers in Nutrition*, *5*. https://doi.org/10.3389/fnut.2018.00087

Daina, A., Michielin, O., & Zoete, V. (2017). SwissADME: A free web tool to evaluate pharmacokinetics, drug-likeness and medicinal chemistry friendliness of small molecules. *Scientific Reports*, *7*(1). https://doi.org/10.1038/srep42717

De Clercq, E., & Li, G. (2016). Approved antiviral drugs over the past 50 years. *Clinical Microbiology Reviews*, *29*(3), 695–747. https://doi.org/10.1128/CMR.00102-15

Elfiky, A. A., & Azzam, E. B. (2020). Novel Guanosine Derivatives against MERS CoV polymerase: An *in silico* perspective. *Journal of Biomolecular Structure and Dynamics*. https://doi.org/10.1080/07391102.2020.1758789

Elmezayen, A. D., Al-Obaidi, A., Şahin, A. T., & Yelekçi, K. (2020). Drug repurposing for coronavirus (COVID-19): *in silico* screening of known drugs against coronavirus 3CL hydrolase and protease enzymes. *Journal of Biomolecular Structure and Dynamics*. https://doi.org/10.1080/07391102.2020.1758791

Enayatkhani, M., Hasaniazad, M., Faezi, S., Guklani, H., Davoodian, P., Ahmadi, N., Einakian, M. A., Karmostaji, A., Ahmadi, K. (2020). Reverse vaccinology approach to design a novel multi-epitope vaccine candidate against COVID-19: An in silico study. *Journal of Biomolecular Structure and Dynamics*. https://doi.org/10.1080/07391102.2020.1756411

Fitchett, J. R., Head, M. G., Cooke, M. K., Wurie, F. B., & Atun, R. (2014). Funding infectious disease research: A systematic analysis of UK research investments by funders 1997-2010. *PLoS One*, *9*(8), e105722. https://doi.org/10.1371/journal.pone.0105722

Ganeshpurkar, A., & Saluja, A. K. (2017). The pharmacological potential of rutin. *Saudi Pharmaceutical Journal*, *25*(2), 149–164. https://doi.org/10.1016/j.jsps.2016.04.025

Gautret, P., Lagier, J.-C., Parola, P., Hoang, V. T., Meddeb, L., Mailhe, M., Doudier, B., Courjon, J., Giordanengo, V., Vieira, V. E., Dupont, H. T., Honoré, S., Colson, P., Chabrière, E., La Scola, B., Rolain, J.-M., Brouqui, P., & Raoult, D. (2020). Hydroxychloroquine and azithromycin as a treatment of COVID-19: Results of an open-label non-randomized clinical trial. *International Journal of Antimicrobial Agents*, 105949. https://doi.org/10.1016/j.ijantimicag.2020.105949

Grosdidier, A., Zoete, V., & Michielin, O. (2011). SwissDock, a protein-small molecule docking web service based on EADock DSS. *Nucleic Acids Research*, *39*(suppl), W270–7. https://doi.org/10.1093/nar/gkr366

Gupta, M. K., Vemula, S., Donde, R., Gouda, G., Behera, L., & Vadde, R. (2020). In-silico approaches to detect inhibitors of the human severe acute respiratory syndrome coronavirus envelope protein ion channel. *Journal of Biomolecular Structure and Dynamics*. https://doi.org/10.1080/07391102.2020.1751300

Hasan, A., Paray, B. A., Hussain, A., Qadir, F. A., Attar, F., Aziz, F. M., Sharifi, M., Derakhshankhah, H., Rasti, B., Mehrabi, M., Shahpasand, K., Saboury, A. A., & Falahati, M. (2020). A review on the cleavage priming of the spike protein on coronavirus by angiotensin-converting enzyme-2 and furin. *Journal of Biomolecular Structure and Dynamics*. https://doi.org/10.1080/07391102.2020.1754293

Jin, Z., Du, X., Xu, Y., Deng, Y., Liu, M., Zhao, Y., … Yang, H. (2020). Structure of Mpro from COVID-19 virus and discovery of its inhibitors. *BioRxiv*, https://doi.org/10.1101/2020.02.26.964882

Jo, S., Kim, S., Shin, D. H., & Kim, M. S. (2020). Inhibition of SARS-CoV 3CL protease by flavonoids. *Journal of Enzyme Inhibition and Medicinal Chemistry*, *35*(1), 145–151. https://doi.org/10.1080/14756366.2019.1690480

Khaerunnisa, S., Kurniawan, H., Awaluddin, R., Suhartati, S. (2020). Potential Inhibitor of COVID-19 Main Protease (M pro) from Several Medicinal Plant Compounds by Molecular Docking Study. *Preprints (Www.Preprints.Org) | NOT PEER-REVIEWED | Posted: 13 March 2020*, https://doi.org/10.20944/Preprints202003.0226.V1 (March), 1–14.

Khan, R. J., Jha, R. K., Amera, G., Jain, M., Singh, E., Pathak, A., … Singh, A. K. (2020). Targeting SARS-CoV-2: A systematic drug repurposing approach to identify promising inhibitors against 3C-like Proteinase and 2′-O-RiboseMethyltransferase. *Journal of Biomolecular Structure & Dynamics*, 1–40. https://doi.org/10.1080/07391102.2020.1753577

Khan, S. A., Zia, K., Ashraf, S., Uddin, R., & Ul-Haq, Z. (2020). Identification of chymotrypsin-like protease inhibitors of SARS-CoV-2 via integrated computational approach. *Journal of Biomolecular Structure and Dynamics*. https://doi.org/10.1080/07391102.2020.1751298

Law, G. L., Tisoncik-Go, J., Korth, M. J., & Katze, M. G. (2013). Drug repurposing: A better approach for infectious disease drug discovery? *Current Opinion in Immunology*, *25*(5), 588–592. https://doi.org/10.1016/j.coi.2013.08.004

Lu, H. (2020). Drug treatment options for the 2019-new coronavirus (2019-nCoV). *BioScience Trends*, *14*(1), 69–71. https://doi.org/10.5582/bst.2020.01020

Lu, H., Stratton, C. W., & Tang, Y. (2020). Outbreak of pneumonia of unknown etiology in Wuhan, China: The mystery and the miracle. *Journal of Medical Virology*, *92*(4), 401–402. https://doi.org/10.1002/jmv.25678

Morse, J. S., Lalonde, T., Xu, S., & Liu, W. R. (2020). Learning from the Past: Possible urgent prevention and treatment options for severe acute respiratory infections caused by 2019-nCoV. *ChemBioChem.*, *21*(5), 730–738. https://doi.org/10.1002/cbic.202000047

Muralidharan, N., Sakthivel, R., Velmurugan, D., & Gromiha, M. M. (2020). Computational studies of drug repurposing and synergism of lopinavir, oseltamivir and ritonavir binding with SARS-CoV-2 protease against COVID-19. *Journal of Biomolecular Structure and Dynamics*. https://doi.org/10.1080/07391102.2020.1752802

Owen, C. D., Lukacik, P., Strain-Damerell, C. M., Douangamath, A., Powell, A. J., Fearon, D., Brandao-Neto, J., Crawshaw, A. D., Aragao, D., Williams, M., Flaig, R., Hall, D. R., McAuley, K. E., Mazzorana, M., Stuart, D. I., von Delft, F., & Walsh, M. A. (2020). COVID-19 main protease with unliganded active site (2019-nCoV, coronavirus disease 2019,

SARS-CoV-2). *RCSB Protein Data Bank (PDB) ID*, *6Y84*, 3–7. https://doi.org/10.2210/pdb6Y84

Panic, G., Duthaler, U., Speich, B., & Keiser, J. (2014). Repurposing drugs for the treatment and control of helminth infections. *International Journal for Parasitology: Drugs and Drug Resistance*, *4*(3), 185–200. https://doi.org/10.1016/j.ijpddr.2014.07.002

Pant, S., Singh, M., Ravichandiran, V., Murty, U. S. N., & Srivastava, H. K. (2020). Peptide-like and small-molecule inhibitors against Covid-19. *Journal of Biomolecular Structure & Dynamics*. https://doi.org/10.1080/07391102.2020.1757510

Park, K. (2019). A review of computational drug repurposing. *Translational and Clinical Pharmacology*, *27*(2), 59–63. https://doi.org/10.12793/tcp.2019.27.2.59

Parvez, M. K., Tabish Rehman, M., Alam, P., Al-Dosari, M. S., Alqasoumi, S. I., & Alajmi, M. F. (2019). Plant-derived antiviral drugs as novel hepatitis B virus inhibitors: Cell culture and molecular docking study. *Saudi Pharmaceutical Journal*, *27*(3), 389–400. https://doi.org/10.1016/j.jsps.2018.12.008

Pettersen, E. F., Goddard, T. D., Huang, C. C., Couch, G. S., Greenblatt, D. M., Meng, E. C., & Ferrin, T. E. (2004). UCSF Chimera—A visualization system for exploratory research and analysis. *Journal of Computational Chemistry*, *25*(13), 1605–1612. https://doi.org/10.1002/jcc.20084

Sarma, P., Sekhar, N., Prajapat, M., Avti, P., Kaur, H., Kumar, S., … Medhi, B. (2020). In-silico homology assisted identification of inhibitor of RNA binding against 2019-nCoV N-protein (N terminal domain). *Journal of Biomolecular Structure & Dynamics*. https://doi.org/10.1080/07391102.2020.1753580

Schrodinger LLC. (2017). The PyMOL Molecular Graphics System, Version 2.0, Schrödinger, LLC.

Thayil, S. M., & Thyagarajan, S. P. (2016). Pa-9: A flavonoid extracted from plectranthus amboinicus inhibits HIV-1 protease. *International Journal of Pharmacognosy and Phytochemical Research*, *8*(6), 1020–1024.

Thompson, M. A. (2004). Molecular docking using ArgusLab, an efficient shape-based search algorithm and the AScore scoring function [Paper presentation].ACS Meeting.

Thuy, B. T. P., My, T. T. A., Hai, N. T. T., Hieu, L. T., Hoa, T. T., Thi Phuong Loan, H., Triet, N. T., Anh, T. T. V., Quy, P. T., Tat, P. V., Hue, N. V., Quang, D. T., Trung, N. T., Tung, V. T., Huynh, L. K., & Nhung, N. T. A. (2020). Investigation into SARS-CoV-2 resistance of compounds in garlic essential oil. *ACS Omega*, *5*(14), 8312–8320. https://doi.org/10.1021/acsomega.0c00772

Vardakas, K. Z., Michalopoulos, A., & Falagas, M. E. (2005). Fluconazole versus itraconazole for antifungal prophylaxis in neutropenic patients with haematological malignancies: A meta-analysis of randomised-controlled trials. *British Journal of Haematology*, *131*(1), 22–28. https://doi.org/10.1111/j.1365-2141.2005.05727.x

Wang, M., Cao, R., Zhang, L., Yang, X., Liu, J., Xu, M., Shi, Z., Hu, Z., Zhong, W., & Xiao, G. (2020). Remdesivir and chloroquine effectively inhibit the recently emerged novel coronavirus (2019-nCoV) in vitro. *Cell Research*, *30*(3), 269–271. https://doi.org/10.1038/s41422-020-0282-0

Wang, Y., Fan, G., Salam, A., Horby, P., Hayden, F. G., Chen, C., Pan, J., Zheng, J., Lu, B., Guo, L., Wang, C., & Cao, B. (2020). Comparative effectiveness of combined favipiravir and oseltamivir therapy versus oseltamivir monotherapy in critically ill patients with influenza virus infection. *The Journal of Infectious Diseases*, *221*(10), 1688–1698. https://doi.org/10.1093/infdis/jiz656

Wu, Y.-S., Lin, W.-H., T.-A.Hsu, J., & Hsieh, H.-P. (2006). Antiviral drug discovery against SARS-CoV. *Current Medicinal Chemistry*, *13*(17), 2003–2020. https://doi.org/10.2174/092986706777584988

Xu, Z., Peng, C., Shi, Y., Zhu, Z., Mu, K., Wang, X., & Zhu, W. (2020). Nelfinavir was predicted to be a potential inhibitor of 2019-nCov main protease by an integrative approach combining homology modelling, molecular docking and binding free energy calculation. *BioRxiv*, p. 2020.01.27.921627. https://doi.org/10.1101/2020.01.27.921627

Zakaryan, H., Arabyan, E., Oo, A., & Zandi, K. (2017). Flavonoids: Promising natural compounds against viral infections. *Archives of Virology*, *162*(9), 2539–2551. https://doi.org/10.1007/s00705-017-3417-y

Zhang, L., Lin, D., Sun, X., Curth, U., Drosten, C., Sauerhering, L., … Hilgenfeld, R. (2020). Crystal structure of SARS-CoV-2 main protease provides a basis for design of improved α-ketoamide inhibitors. *Science*, eabb3405. https://doi.org/10.1126/science.abb3405